

## Spectral and Biological Studies on New Mixed Ligand Complexes

T. K. Pal<sup>1\*</sup>, M. A. Alam<sup>1</sup>, J. Hossen<sup>1</sup>, S. Paul<sup>2</sup>, H. Ahmad<sup>3</sup>, M. C. Sheikh<sup>4</sup>

<sup>1</sup>Department of Chemistry, Rajshahi University of Engineering & Technology, Dhaka, Bangladesh

<sup>2</sup>Department of Pharmacy, University of Rajshahi, Dhaka, Bangladesh

<sup>3</sup>Department of Chemistry, University of Rajshahi, Dhaka, Bangladesh

<sup>4</sup>Department of Applied Chemistry, University of Toyama, Japan

Received 13 April 2018, accepted in final revised form 17 May 2018

### Abstract

In this study, new mixed ligand complexes have been prepared from bis(2,4,4-trimethylpentyl)dithiophosphinic acid (C<sub>16</sub>H<sub>35</sub>PS<sub>2</sub>) and 2,9-dimethyl-1,10-phenanthroline (C<sub>14</sub>H<sub>12</sub>N<sub>2</sub>) with various metal(II) ions. The molecular formula of the metal complexes were [Mn(C<sub>16</sub>H<sub>34</sub>PS<sub>2</sub>)(C<sub>14</sub>H<sub>12</sub>N<sub>2</sub>)]Cl (**1**), [Fe(C<sub>16</sub>H<sub>34</sub>PS<sub>2</sub>)(C<sub>14</sub>H<sub>12</sub>N<sub>2</sub>)]Cl (**2**), [Co(C<sub>16</sub>H<sub>34</sub>PS<sub>2</sub>)(C<sub>14</sub>H<sub>12</sub>N<sub>2</sub>)]Cl (**3**), [Zn(C<sub>16</sub>H<sub>34</sub>PS<sub>2</sub>)(C<sub>14</sub>H<sub>12</sub>N<sub>2</sub>)]Cl (**4**) and [Cd(C<sub>16</sub>H<sub>34</sub>PS<sub>2</sub>)(C<sub>14</sub>H<sub>12</sub>N<sub>2</sub>)]Cl (**5**). These complexes have been characterized by various physico-chemical techniques such as melting point, molar conductance, magnetic susceptibility measurements as well as UV-Vis, IR, TG and mass spectroscopic analyses. The surface morphology was determined by scanning electron microscope (SEM). The magnetic moment value, color as well as spectral measurements suggested that the geometrical structures of the metal complexes were tetrahedral. The spectral data showed that bis(2,4,4-trimethylpentyl)dithiophosphinic acid and 2,9-dimethyl-1,10-phenanthroline ligands acted as uninegative and neutral bidentate ligand, respectively. The obtained mixed ligand complexes were more stable in air and highly soluble in common organic solvent. The bio-efficacy of ligands and metal complexes have been screened against the test microorganism using agar disc diffusion method. The complex **4** showed potential antibacterial activity against *Sterptococcus aureus* as compared to standard drug, imipenem. On the other hand, the complex **3** also displayed more potent antifungal activity against *Lecanicillium fungicola*. Moreover, the complex **3** was also found to have better scavenging activity against 2,2-diphenyl-1-picrylhydrazyl.

**Keywords:** Bis(2,4,4-trimethylpentyl)dithiophosphinic acid; SEM; Antioxidant.

© 2018 JSR Publications. ISSN: 2070-0237 (Print); 2070-0245 (Online). All rights reserved.  
doi: <http://dx.doi.org/10.3329/jsr.v10i3.36379>

J. Sci. Res. **10** (3), 291-302 (2018)

## 1. Introduction

Bis(2,4,4-trimethylpentyl)dithiophosphinic acid (BDTPA) is sulfur substitution of organo-phosphorous extracting reagent. Sulfur has lower electronegativity as compared to

---

\* Corresponding author: [tkpchem@gmail.com](mailto:tkpchem@gmail.com)

oxygen. Thus electrons of sulfur atom are more easily shared in the formation of metal-sulfur bond and increase the bond strength. BDTPA has been widely used as reagent for the extraction of trace metals in sample [1]. As a ligand, 2,9-dimethyl-1,10-phenanthroline (DMP) is a bidentate heterocyclic nitrogenous species. Attached methyl groups have tendency to donate electrons to the group/atom attached to them. Thus lone pair electrons on nitrogen atoms of DMP can easily bond with metal ion and form five-membered ring structure. DMP has potential complexation, chemotherapy, catalytic, and biological activities. DMP had been used as an analytical reagent in both analytical and coordination chemistry. Complexes containing 2,9-dimethyl-1,10-phenanthroline applied as photovoltaic cells and molecular sensors [2–4] as well as these complexes have been showed potent DNA binding affinity, DNA cleavage ability and higher cytotoxicity against human MCF-7 breast cancer cell line [5,6]. Moreover, mixed ligand complexes containing heterocyclic nitrogenous ligands have a unique role in drug industry and potential applications in various fields, e.g. as promising antitumor activity [7], anticancer [8], antifungal, antibacterial [9], antioxidant [10], antimycoplasmal activity [11] as well as coordination polymers, corrosion inhibitors, optical materials and solar cell dyes [10]. Numerous metal complexes with 2,9-dimethyl-1,10-phenanthroline as a ligand or mixed with other ligands were reported [12–15]. As a continuation of research in this area, we report herein the synthesis, characterization and biological study of mixed ligand complexes with bis(2,4,4-trimethylpentyl)dithiophosphinic acid and 2,9-dimethyl-1,10-phenanthroline. The mixed ligand complexes were found to have the general formula  $[M(C_{16}H_{34}PS_2)(C_{14}H_{12}N_2)]Cl$  ( $M = Mn(II), Fe(II), Co(II), Zn(II)$  or  $Cd(II)$ ).

## 2. Materials and Methods

All chemicals were analytical grade reagents from Merck and Sigma Aldrich and used without further purification. IR spectra were recorded on an IR Affinity 1S spectrophotometer, Shimadzu, Japan with samples prepared as KBr pellets. UV–Visible absorption spectra were recorded on a T60 UV-Visible spectrophotometer (PG Instruments, UK) programmed with Win5 software, version 5.1. The Mass spectra were obtained on a JEOL-JMS-D300 spectrometer. Thermogravimetric analysis was carried out on a TG 60, Shimadzu, at a heating rate of  $10\text{ }^\circ\text{C min}^{-1}$  from room temperature to  $800\text{ }^\circ\text{C}$  under nitrogen gas. The percentage mass loss was recorded against the temperature. Magnetic susceptibility and molar conductance measurements were made on a magnetic susceptibility balance (Sherwood Scientific, UK) and an ECOSCAN CON5 conductivity/temperature meter (Eutech Instruments, Singapore, Serial No. 101886), respectively. Particle size and surface morphology were observed on a JEOL, JSM-6360 LV with energy-diffusive X-ray spectroscopy JEOL, JED-2300.

### 2.1. General procedure for synthesis of mixed ligand complexes

The appropriate quantity of hot saturated methanolic solution of metal chloride salt (1 mmol, 0.198 g of  $MnCl_2 \cdot 4H_2O$ , 0.235 g of  $FeCl_2 \cdot 6H_2O$ , 0.238 g of  $CoCl_2 \cdot 6H_2O$ , 0.136 g of

ZnCl<sub>2</sub> or 0.228 g of CdCl<sub>2</sub>·2.5H<sub>2</sub>O) was added in methanolic solution of 2,9-dimethyl-1,10-phenanthroline (1 mmol, 0.208 g) with continuous stirring at 60 °C. To this resulting solution a hot saturated methanolic solution of bis(2,4,4-trimethylpentyl)dithiophosphinic acid (1 mmol, 0.322 g) was added. The solution was refluxed at 100 °C with continuous stirring whereupon the complex was precipitated. The precipitate was separated by filtration and washed several times with hot methanol. The complexes were purified by recrystallization from methanol solution. Finally, pure complexes were dried in vacuum over anhydrous calcium chloride. The purity of the complexes was verified using thin-layer chromatography (TLC).

## 2.2. DPPH free radical scavenging ability

The antioxidant activity of the mixed ligand complexes (**1-5**) was determined by DPPH method [16,17]. 2 mL of various concentrations of the samples (31.25, 62.50, 125, 250 and 500 µg) was added to 2 mL of 0.004 % chloroformic solution of DPPH. The samples were vortexed and incubated in the dark place for 30 min at room temperature. The absorbance was measured against a blank at 517 nm. Butylated hydroxyl toluene (BHT) was used as a standard for comparison. The assay was carried out in triplicate and the mean was reported. The DPPH radical scavenging activity was calculated by the following equation:

$$\text{DPPH radical scavenging activity (\%)} = [(A_{\text{control}} - A_{\text{sample}})/A_{\text{control}}] \times 100$$

Where  $A_{\text{control}}$  is the absorbance of reaction without sample and  $A_{\text{sample}}$  is the absorbance of test sample. Sample concentration providing 50% inhibition ( $IC_{50}$ ) was calculated from the graph.

## 2.3. Antibacterial and antifungal screening

The antimicrobial activity of ligands and their mixed ligand complexes (**1-5**) was screened against *Sterptococcus pneumoniae* (*S. pneumoniae*), *Bacillus subtilis* (*B. subtilis*), *Staphylococcus aureus* (*S. aureus*), *Staphylococcus epidermidis* (*S. epidermidis*) and *Clostridium botulinum* (*C. botulinum*) bacteria and *Aspergillus flavus* (*A. flavus*), *Lecanicillium fungicola* (*L. fungicola*) and *Aspergillus niger* (*A. niger*) fungi species using disc diffusion method [15,18,19]. The stock solution (1 mg/mL) of the sample was prepared by dissolving 10 mg of the test compound in 10 mL of chloroform. Control was prepared by solvent instead of stock solution. Sterile media was poured into sterilized petri dishes and allowed to settle for 15 min. Then 100 µL of microorganism was inoculated on media with the help of micropipette. Later on, the sample was placed on the filter disc. Diameter of filter disc was 4 mm. The petri dishes were incubated at 37 °C for 24 h in case of bacteria and 48 h at 30 °C for fungal strains. Standard antibacterial drug (imipenem) and antifungal drug (fluconazole) were also screened under similar condition for comparison. In order to clarify any effect of chloroform on the biological screening,

separate study was carried out only in chloroform. The zone of inhibition was measured in mm and average zone inhibition was determined. Duplicate data was taken for the calculation of mean inhibition.

### 3. Results and Discussion

#### 3.1. Molar conductivity and nature of species

The molar conductance values of metal complexes were found to be in the range 82-102  $\text{ohm}^{-1}\text{cm}^2\text{mol}^{-1}$  ( Table 1) suggesting 1:1 electrolyte as well as ionic in nature due to the presence of one chloride ion in the outside of coordination sphere [20,21]. The results reveal that the isolated mixed ligand complexes were 1:1:1 (L: M: L) ratio. Melting point gives primary information about the formation of complex. The higher melting point of the prepared complexes (200-271 °C) as compared to ligand indicating the formation of metal complexes [22,23]. The sharp melting point indicated the purity of metal complexes. Mixed ligand complexes were soluble in most common solvents like acetonitrile, chloroform, dichloromethane, DMF and toluene. The experimental physico-chemical data of the metal complexes were in good agreement with the proposed structural formula.

Table 1. Physical properties of the ligands and mixed ligand complexes.

Ligand/Complex	Color	Melting point ( $\pm 2$ °C)	Yield (%)	$\Lambda$ ( $\text{ohm}^{-1}\text{cm}^2\text{mole}^{-1}$ )
DMP	Light beige	166	-	-
BDTPA	Greenish liquid	-	-	-
1	Green	253	52	102
2	Coffee	201	43	86
3	Blue	200	40	91
4	White	265	51	82
5	White	271	55	88

#### 3.2. IR spectra and mode of bonding

The infrared spectra gives important information about the nature of functional groups and binding mode of ligand to metal ion in complex. The characteristic absorption bands in the IR spectra were represented in Table 2. A medium band at  $1654\text{ cm}^{-1}$  was attributed to stretching mode of the C=N in 2,9-dimethyl-1,10-phenanthroline [24–27]. This band was shifted to lower frequency (30-38) in the complexes which clearly indicated the coordination of the two nitrogen atoms with metal ion. The new peaks in the region  $511\text{--}544\text{ cm}^{-1}$  can be assigned to asymmetric stretching M-N in metal complexes proving the coordination of the 2,9-dimethyl-1,10-phenanthroline as bidentate cleating agent [28–31]. The bands at  $2866\text{--}2868$  and  $2901\text{--}2957\text{ cm}^{-1}$  can be attributed to symmetric and asymmetric stretching mode of C-H, respectively [32]. In mixed ligand complexes the

characteristic bands of  $\nu(\text{C-H})$  were almost same, as expected. This further informed that these parts did not participate in coordination. The free bis(2,4,4-trimethylpentyl)dithiophosphinic acid showed a medium band at  $2638\text{ cm}^{-1}$  for  $\nu(\text{S-H})$  vibration [33]. This band was found to have disappeared in respective complexes confirming the coordination of sulfur atom with metal ion *via* deprotonation. A medium band of  $\nu(\text{P=S})$  was observed at  $637\text{ cm}^{-1}$  [1,33,34]. This band was shifted to lower frequency ( $24\text{-}37\text{ cm}^{-1}$ ) in metal complexes. In this case, sulphur atom of thiophosphoryl group coordinated with metal ions due to the donation of electrons from sulphur to the empty *d*-orbitals of metal ions. In addition, the weak peak in the region of  $419\text{-}426\text{ cm}^{-1}$  was assigned to stretching vibrations of M-S bond confirming the coordination of sulfur atoms of bis(2,4,4-trimethylpentyl)dithiophosphinic acid with metal ion as uninegative bidentate fashion [1,24].

Table 2. Selected infrared absorption frequencies ( $\text{cm}^{-1}$ ) of ligands and their metal complexes.

Ligand /complex	$\nu(\text{C=N})$	$\nu(\text{P=S})$	$\nu(\text{S-H})$	$\nu(\text{M-S})$ & $\nu(\text{M-N})$
BDTPA	-	637	2638	-
DMP	1654	-	-	-
1	1622	607	-	419 & 540
2	1616	613	-	419 & 516
3	1622	609	-	419 & 544
4	1624	601	-	426 & 527
5	1620	600	-	420 & 511

### 3.3. Electronic spectra and magnetic properties

The electronic spectra provide feasible indication about the ligand arrangement in metal complexes. It also distinguishes among the square-planar, tetrahedral and octahedral geometries of complex. Magnetic moment value gives reliable information about paramagnetic or diamagnetic nature as well as geometry of complex. Color further assists to find out the correct geometry of the complexes [35]. The ligand (DMP) showed two bands at 265 nm and 295 nm, which ascribed to transitions  $\pi \rightarrow \pi^*$  and  $n \rightarrow \pi^*$ , respectively. An absorption peak of BDTPA exhibited at 260 nm and 290 nm, which assigned to  $\pi \rightarrow \pi^*$  and  $n \rightarrow \pi^*$  transitions, respectively. These bands were shifted towards shorter wavelength region in the spectra of metal complexes which is an evidence of coordination of ligand to metal ions [36]. The UV-visible spectroscopic data, color and magnetic moment values of the test compounds are listed in Table 3. Complex **1** exhibited one absorption band at 582 nm which assigned to  ${}^6\text{A}_1 \rightarrow {}^4\text{T}_1$  transition due to tetrahedral geometry. The magnetic moment and green color of the complex are an additional evidence for tetrahedral structure [37,38]. The high-spin complex **2** showed a weak band at 527 nm owing to  ${}^5\text{T}_2 \rightarrow {}^5\text{E}$  transition. In addition, the magnetic moment value as well as yellow color of the complex ascribed for tetrahedral geometry [39,40]. The four coordinated complex **3** displayed two peaks at 471 nm and 684 nm, assigned to

${}^4T_2(F) \rightarrow {}^4T_1(P)$  transition. The magnetic moment value and blue color of the complex are consistent with tetrahedral stereochemistry [41–43]. Metal complexes with white color (**4** and **5**) did not show d-d electronic transition due to completely filled  $d^{10}$ -orbital [41]. According to magnetic moment value, complex **1-3** were paramagnetic while **2** and **3** were diamagnetic in nature.

Table 3. Electronic spectra, magnetic moments and geometry of ligands/metal complexes.

Ligand/Complex	Band (nm)	$\epsilon$ (Lmol <sup>-1</sup> cm <sup>-1</sup> )	Assignments	$\mu_{\text{eff}}$ (BM)	Geometry
BDTPA	260	3275	$\pi \rightarrow \pi^*$	-	-
	290	2691	$n \rightarrow \pi^*$	-	-
DMP	265	3081	$\pi \rightarrow \pi^*$	-	-
	295	2863	$n \rightarrow \pi^*$	-	-
1	230	935	$\pi \rightarrow \pi^*$	5.73	Tetrahedral
	270	811	$n \rightarrow \pi^*$		
	582	56	${}^6A_1 \rightarrow {}^4T_1$		
2	230	1658	$\pi \rightarrow \pi^*$	5.19	Tetrahedral
	265	1621	$n \rightarrow \pi^*$		
	527	126	${}^5T_2 \rightarrow {}^5E$		
3	235	2696	$\pi \rightarrow \pi^*$	4.38	Tetrahedral
	265	2808	$n \rightarrow \pi^*$		
	529	130	${}^4T_2(F) \rightarrow {}^4T_1(P)$		
4	239	1456	$\pi \rightarrow \pi^*$	Diamagnetic	Tetrahedral
	275	2064	$n \rightarrow \pi^*$		
5	230	1392	$\pi \rightarrow \pi^*$	Diamagnetic	Tetrahedral
	270	1217	$n \rightarrow \pi^*$		

### 3.4. Thermal analysis

Thermogravimetric analysis is a powerful tool to confirm both the composition and stability of the complexes. Fig.1 represents the proposed chemical change as a function of temperature and corresponding mass loss in each step. 2,9-dimethyl-1,10-phenanthroline was decomposed progressively in two steps. The first mass loss of DMP occurred in the range 256 to 327 °C having mass loss 12.56% due to elimination  $C_2H_2$  (cal 12.50). The second mass loss happened in the range of 328 to 544°C due to deduction of  $5C_2H_2$  and  $C_2N_2$  molecules with a found mass loss of 87.44% (cal 87.50%). All metal complexes were decomposed progressively in three steps with almost same trend. In complex **1** the first mass loss occurred in the range 277 to 327°C having mass loss of 5.75% due to the elimination of  $0.5Cl_2$  molecule (cal 5.65%). The second degradation step happened in the range of 328 to 386 °C with mass loss of 33.58% (cal 33.61%) corresponding to loss of  $6C_2H_2$  and  $C_2N_2$  species. The third step occurred in the range 387 to 574 °C with mass loss of 46.67% (cal 46.71%) due to the deduction of  $C_2H_2$ ,  $7C_2H_4$ ,  $PH_3$  and  $H_2S$  molecules. Finally, 14.00% (cal 14.04%) metallic residue remained as MnS. The first

thermal decomposition of complex **2** ensued in the range of 70 to 203 °C with mass loss of 5.70% (cal 5.64%) due to the elimination of 0.5Cl<sub>2</sub> molecule. The second step occurred in the range of 204 to 284 °C with mass loss of 33.53% (cal 33.55%) corresponding to the loss of 6C<sub>2</sub>H<sub>2</sub> and C<sub>2</sub>N<sub>2</sub> moiety. Third step happened due to the loss of C<sub>2</sub>H<sub>2</sub>, 7C<sub>2</sub>H<sub>4</sub>, PH<sub>3</sub> and H<sub>2</sub>S molecules with a found mass loss of 46.61% (cal 46.63%) in the range of 285 to 480°C followed by the formation of 14.16% FeS (cal 14.17%). In complex **3** the first mass loss ensued in the range 92 to 202 °C with mass loss of 5.66% (cal 5.62%) corresponding to the deduction of 0.5Cl<sub>2</sub> molecule. The second step decomposition occurred in the range of 203 to 318°C due to the loss of 6C<sub>2</sub>H<sub>2</sub> and C<sub>2</sub>N<sub>2</sub> species with mass loss of 33.38% (cal 33.39%). The third step occurred in the range of 319 to 491 °C with mass loss of 46.39% (cal 46.41%) due to the loss of C<sub>2</sub>H<sub>2</sub>, 7C<sub>2</sub>H<sub>4</sub>, PH<sub>3</sub> and H<sub>2</sub>S molecules, leading finally stable 14.57% CoS as residue (cal 14.45%). The first decomposition of complex **4** occurred in the temperature range of 257 to 305 °C with mass loss of 5.63% (cal 5.57%) corresponding to the loss of 0.5Cl<sub>2</sub> molecule. Second decomposition step happened in the temperature range 306 to 368 °C with mass loss of 33.11% (cal 33.13%) due to the loss of 6C<sub>2</sub>H<sub>2</sub> and C<sub>2</sub>N<sub>2</sub> species. Third decomposition step occurred in the temperature range 369 to 606 °C with mass loss of 46.02% (cal 46.04%) corresponding to the loss of C<sub>2</sub>H<sub>2</sub>, 7C<sub>2</sub>H<sub>4</sub>, PH<sub>3</sub> and H<sub>2</sub>S molecules leading finally to the most stable species zinc sulphide as residual product (Found 15.24; cal 15.27%). The first step of complex **5** occurred in the range 232 to 303 °C having mass loss of 5.18% (cal 5.16%) due to the elimination of 0.5Cl<sub>2</sub> molecule. The second degradation step happened in the range of 304 to 412 °C with mass loss of 30.66% (cal 30.69%) corresponding to loss of 6C<sub>2</sub>H<sub>2</sub> and C<sub>2</sub>N<sub>2</sub> species. The third step occurred in the temperature range of 413 to 694 °C with mass loss of 42.62% (cal 42.65%) due to the deduction of C<sub>2</sub>H<sub>2</sub>, 7C<sub>2</sub>H<sub>4</sub>, PH<sub>3</sub> and H<sub>2</sub>S molecules. Finally, 21.54% (cal 21.51%) metallic residue remained as CdS. The experimental molecular mass of metal complexes were in good agreement with suggested molecular formula.

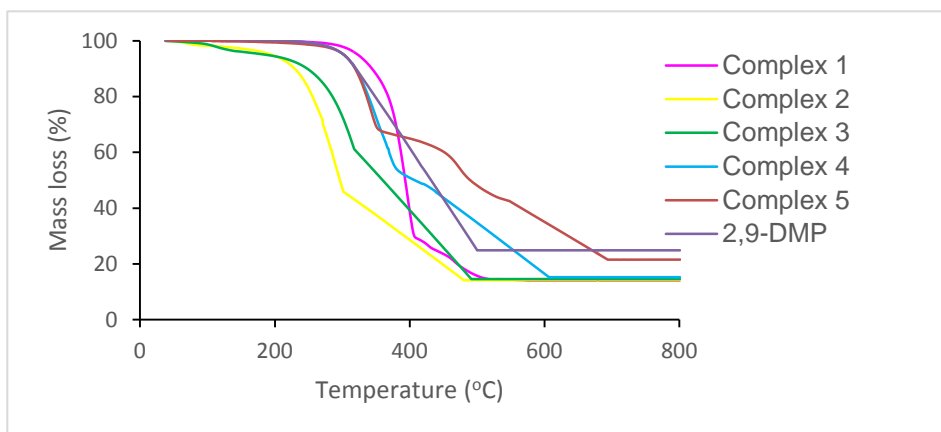


Fig. 1. TG spectra for the ligand (DMP) and metal complexes.

### 3.5. FAB-mass spectra

The data of mass spectroscopic analysis are presented in Table 4. The molecular ion peak of metal complex **1-5** was appeared in the FAB mass spectra at  $m/z = 620.7$ ,  $m/z = 621.1$ ,  $m/z = 623.8$ ,  $m/z = 629.0$  and  $m/z = 677.4$ , respectively. Moreover, complex **1-5** showed another characteristic peak at  $m/z = 585.7$ ,  $m/z = 586.1$ ,  $m/z = 588.8$ ,  $m/z = 594.0$  and  $m/z = 642.5$ , respectively due to the loss of one chloride ligand [44-46]. Both molecular ion and characteristic peak of metal complexes were in good agreement with their assigned molecular formula. This further confirmed that the mixed ligand complexes were 1:1 ratio as well as mononuclear composition.

Table 4. Characteristic peaks of FAB-mass spectrum of the mixed ligand complexes.

Complex	$[M]^+$	$[M-Cl]^+$	$[M-C_{16}H_{34}PS_2Cl]^+$	$[C_{10}H_{10}N_2]$
1	620.7	585.7	266.2	158.8
2	621.1	586.1	265.9	158.8
3	623.8	588.8	268.2	158.8
4	629.0	594.0	273.4	158.8
5	677.4	642.5	322.0	158.8

### 3.6. Scanning electron microscopy

The surface morphology is one of the characteristics of solid materials. The scanning electron microscope (SEM) was used to evaluate the morphology and particle size of sample. A beam of high-energy electrons of scanning electron microscope creates a variety of signals from the surface of solid matter. These signals provide information about the image of the shape, size of the particles, ductility of substances, strength of materials and how the atoms are arranged in an object. The scanning electron microscope can be as essential tool in metallurgy, forensic science, gemology as well as medical science. From the SEM photographs, the morphology of ligand (DMP) was homogeneously distributed in solid powder. On the other hand, morphology of respective metal complexes was not uniformly distributed and exhibited different structures. The SEM micrographs showed complexes **1**, **2**, **3** and **4** seemed to be spherical like structure with the particle size approximately 197, 151, 181 and 167  $\mu m$ , respectively. Besides, complex **5** showed gravel like structure.

### 3.7. Antioxidant activity

Free radicals generate during normal cellular function in body system. Free radicals (such as superoxide anion, hydroxyl radical and hydrogen peroxide) are very reactive. Because of that they interact with proteins, lipids and nucleic acids, may produce various chronic diseases. Therefore, to obstruct the free radical damage in body system, it is important to control drugs that may be rich in antioxidant. Antioxidants have the ability to scavenge free radicals or terminate chain reactions. They play an important role in repairing cellular



damage and preventing various human diseases. The scavenging free radical ability of metal complexes is an important property [36,47]. Recently to protect the resultant damage, numerous natural as well as synthetic free radical scavengers have been developed and studied [22,47]. The newly synthesized mixed ligand complexes were investigated for their antioxidant properties by DPPH radical scavenging method. 1,1-diphenyl-2-picrylhydrazyl (DPPH) shows a strong absorption band at 517 nm due to its odd electron. An antioxidant reacts with it and produces stable 1,1-diphenyl-2-picrylhydrazine. As a result, the band intensity of DPPH decreases [48]. Table 5 and Fig.2 demonstrate the free radical scavenging activity of metal complexes and BHT. The decreasing absorbance as well as the lower IC<sub>50</sub> value indicated the higher antioxidant activity of test compounds [49-51]. The IC<sub>50</sub> value of test compounds in descending order was **5** > **1** > **4** > BHT > **2** > **3**. Complex **1**, **4** and **5** showed poor scavenging activity as compared to BHT. The free radical scavenging activity of complex **2** was lower than that of **3**, but better than standard antioxidant (BHT). Moreover, complex **3** was found to have better scavenging activity as compared to the standard antioxidant.

Table 5. DPPH free radical scavenging activity of metal complexes.

	Compounds					
	<b>1</b>	<b>2</b>	<b>3</b>	<b>4</b>	<b>5</b>	BHT
IC <sub>50</sub> (ppm)	2.03	1.58	1.57	1.98	2.41	1.75
R <sup>2</sup>	0.927	0.943	0.969	0.949	0.793	0.958

R<sup>2</sup>: correlation coefficient

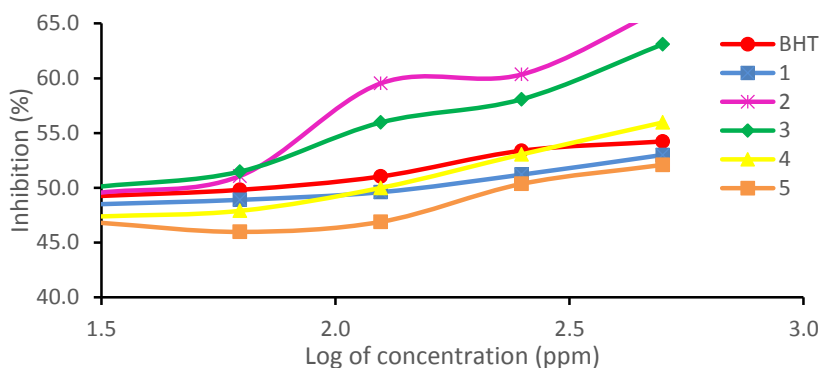


Fig. 2. Antioxidant activity for metal complexes.

### 3.8. Antibacterial and antifungal activity

The antimicrobial activity of the complexes are presented in Table 6. Both bis(2,4,4-trimethylpentyl)dithiophosphinic acid and 2,9-dimethyl-1,10-phenanthroline ligands did not show any activity against test microorganisms. Complexes **2**, **3** and **4** exhibited moderate activity against *Staphylococcus aureus*, *Clostridium botulinum* and *Bacillus*

*subtilis*. In addition, complex **4** showed potent antibacterial activity against *Sterptococcus aureus* as compared to standard, imipenem. The remaining metal complexes showed low activity against all bacterial strains. In the case of antifungal study complex **3** was found to be more potentially active against *Lecanicillium fungicola*. Besides, complex **4** exhibited promising activity against *Aspergillus niger* as compared to standard drug, fluconazol. The biological activity of metal complexes depend on the molecular structure, number of chelate rings, polarity of metal complexes, etc. Only lipid soluble substances can pass through the lipid membrane of microorganism. In the present study some mixed ligand complexes showed less activity due to the lower lipophilicity of the complexes. Because of that the metal complexes could neither block nor inhibit the growth of the microorganisms. While some mixed ligand complexes displayed greater activity than ligands. The increasing activity of mixed ligand complexes can be explained by chelation theory [35]. The lipophilic nature increased in mixed ligand complexes due to chelation. Therefore, the chelation could increase the ability of metal complex to penetrate through the lipid membrane of test microorganism.

Table 6. Antimicrobial activity of the mixed ligand complexes.

Complex /Standard	Zone of inhibition (mm) against bacteria					Zone of inhibition (mm) against fungi		
	<i>S. pneumonia</i>	<i>B. subtilis</i>	<i>S. aureus</i>	<i>S. epidermidi</i>	<i>Clostridium</i>	<i>A. flavus</i>	<i>L. fungicola</i>	<i>A. niger</i>
1	07	08	08	08	09	06	05	05
2	07	9	12	08	08	05	08	10
3	08	09	07	07	16	06	15	05
4	07	12	23	09	08	06	07	13
5	09	07	09	08	05	06	05	06
Imipenem	29	26	28	25	28	-	-	-
Fluconazole	-	-	-	-	-	15	17	16

#### 4. Conclusion

In this paper five new mixed ligand complexes have been successfully synthesized and characterized by various physico-chemical techniques. Based on the experimental data the bis(2,4,4-trimethylpentyl)dithiophosphinic acid acted as uninegative bidentate ligand. The conductance values reveal that the mixed ligand complexes were 1:1 electrolyte in nature. Magnetic moment, color, UV-Vis spectral, mass and TG observation suggested tetrahedral geometry of all metal complexes. Thermally the mixed ligand complexes were more stable. Moreover, complex **4** showed strong antibacterial activity against *Staphylococcus aureus*. Besides, complex **3** and **4** exhibited good activity against *Lecanicillium fungicola* and *Aspergillus niger* fungi species, respectively.

## References

1. T. K. Pal, M. A. Alam, M. A. A. A. Islam, and S. R. Paul, *J. Sci. Res.* **4**, 427 (2012).  
<https://doi.org/10.3329/jsr.v4i2.9366>
2. N. Shahabadi, F. Darabi, M. Maghsudi, and S. Kashanian, *DNA Cell Biol.* **29**, 329 (2010).  
<https://doi.org/10.1089/dna.2009.1001>
3. A. Srivastava, K. Srivastava, and J. Prasad, *J. Appl. Chem.* **5**, 1286 (2016).
4. S. Shabaan, B. Letafat, N. Esmati, A. Shafiee, and F. Alireza, *Asian J. Chem.* **24**, 2819 (2012).
5. L. Kucková, K. Jomová, A. Švorcová, M. Valko, P. Segl'a, J. Moncol', and J. Kožíšek, *Molecules* **20**, 2115 (2015). <https://doi.org/10.3390/molecules20022115>
6. M. Ganeshpandian, S. Ramakrishnan, M. Palaniandavar, E. Suresh, A. Riyasdeen, and M. A. Akbarsha, *J. Inorg. Biochem.* **140**, 202 (2014). <https://doi.org/10.1016/j.jinorgbio.2014.07.021>
7. D. J. Awad, F. Conrad, A. Koch, U. Schilde, A. Pöpl, and P. Strauch, *Inorg. Chim. Acta* **363**, 1488 (2010). <https://doi.org/10.1016/j.ica.2010.01.021>
8. S. Tosonian, C. J. Ruiz, A. Rios, E. Frias, and J. F. Eichler, *Open J. Inorg. Chem.* **13**, 7 (2013).  
<https://doi.org/10.4236/ojic.2013.31002>
9. A. C. Ekennia, D. C. Onwudiwe, A. A. Osowole, L. O. Olasunkanmi, and E. E. Ebenso, *J. Chem.* **2016**, 1 (2016). <https://doi.org/10.1155/2016/5129010>
10. H. Al-N. Taghreed, H. G. Faiza, and S. k. Aliea, *Adv. Phys. Theor. Appl.* **29**, 5 (2014).
11. L. Tabrizi, P. McArdle, M. Ektefan, and H. Chiniforoshan, *Inorg. Chim. Acta* **439**, 138 (2016). <https://doi.org/10.1016/j.ica.2015.10.015>
12. J. H. Pandya, R. N. Jadeja, and K. J. Ganatra, *J. Saudi Chem. Soc.* **18**, 190 (2014).  
<https://doi.org/10.1016/j.jscs.2011.06.010>
13. Q. Y. Zhu and J. Dai, *Coord. Chem. Rev.* **330**, 95 (2017).  
<https://doi.org/10.1016/j.ccr.2016.08.009>
14. A. Crispini, C. Cretu, D. Aparaschivei, A. A. Anedelescu, V. Sasca, V. Badea, I. Aiello, E. I. Szerb, and O. Costisor, *Inorg. Chim. Acta* **470**, 242 (2018).  
<https://doi.org/10.1016/j.ica.2017.05.064>
15. G. C. Zong, N. Ren, J. J. Zhang, X. X. Qi, and J. Gao, *J. Therm. Anal. Calorim.* **123**, 105 (2016). <https://doi.org/10.1007/s10973-015-4901-9>
16. B. Bozin, N. Mimica-Dukic, N. Simin, and G. Anackov, *J. Agric. Food Chem.* **54**, 1822 (2006). <https://doi.org/10.1021/jf051922u>
17. N. Tabassam, S. Ali, S. Shahzadi, M. Shahid, M. Abbas, Q. M. Khan, S. K. Sharma, and K. Qanungo, *Russ. J. Gen. Chem.* **83**, 2423 (2013). <https://doi.org/10.1134/S1070363213120396>
18. E. H. Ismail, D. Y. Sabry, H. Mahdy, and M. M. H. Khalil, *J. Sci. Res.* **6**, 509 (2014).  
<https://doi.org/10.3329/jsr.v6i3.18750>
19. T.R. Allaka, N. Polkam, P. Rayam, J. Sridhara, N.S. Garikapati, S.S. Kotapalli, R. Ummanni, and J. S. Anireddy, *Med. Chem. Res.* **25**, 977(2016). <https://doi.org/10.1007/s00044-016-1544-8>
20. S. Chandra and S. Verma, *Spectrochim. Acta Part A* **71**, 458 (2008).  
<https://doi.org/10.1016/j.saa.2007.10.057>
21. M. M. H. Khalil, E. H. Ismail, G. G. Mohamed, E. M. Zayed, and A. Badr, *Open J. Inorg. Chem.* **2**, 13 (2012). <https://doi.org/10.4236/ojic.2012.22003>
22. A. Olanrewaju, T. I. Oni, and A. A. Osowole, *Chem. Res. J.* **1**, 90 (2016).
23. M. S. Hasan, R. Kayesh, F. Begum, and S. M. A. Rahman, *J. Anal. Methods Chem.* **2016**, 1 (2016). <https://doi.org/10.1155/2016/3560695>
24. D. C. Onwudiwe, Y. B. Nthwane, A. C. Ekennia, and E. Hosten, *Inorg. Chim. Acta* **447**, 134 (2016). <https://doi.org/10.1016/j.ica.2016.03.033>
25. M. A. Mahmoud, S. A. Zaitone, A. M. Ammar, and S. A. Sallam, *J. Mol. Struct.* **1108**, 60 (2016). <https://doi.org/10.1016/j.molstruc.2015.11.055>
26. B. Anupama, A. Aruna, V. Manga, S. Sivan, M. V. Sagar, and R. Chandrashekar, *J. Fluoresc.* **27**, 953 (2017). <https://doi.org/10.1007/s10895-017-2030-5>

27. X. Qi, N. Ren, D. Zhang, and J. Zhang, *Chem. Res. Chinese Univ.* **31**, 1039 (2015). <https://doi.org/10.1007/s40242-015-5052-z>
28. K. Singh, R. Thakur, and V. Kumar, *Beni-Suef Univ. J. Basic Appl. Sci.* **5**, 21 (2016). <https://doi.org/10.1016/j.bjbas.2016.02.001>
29. S. A. Sadeek and S. M. Abd El-Hamid, *J. Therm. Anal. Calorim.* **124**, 547 (2016). <https://doi.org/10.1007/s10973-015-5057-3>
30. K. Mounika, B. Anupama, J. Pragathi, and C. Gyanakumari, *J. Sci. Res.* **2**, 513 (2010). <https://doi.org/10.3329/jsr.v2i3.4899>
31. M. A. Islam, M. A. Mumit, T. K. Pal, and M. A. Alam, *J. Sci. Res.* **4**, 635 (2012). <https://doi.org/10.3329/jsr.v4i3.9807>
32. S. Bal, S. S. Bal, A. Erener, H. Halipci, and S. Akar, *Chem. Pap.* **68**, 352 (2014). <https://doi.org/10.2478/s11696-013-0465-y>
33. T. K. Pal, M. A. Alam, and S. R. Paul, *J. Bangl. Acad. Sci.* **34**, 153 (2010).
34. E. G. Saglam, *Inorg. Chim. Acta* **434**, 188 (2015). <https://doi.org/10.1016/j.ica.2015.05.028>
35. W. H. Mahmoud, G. G. Mohamed, and S. Y. A. Mohamedin, *J. Therm. Anal. Calorim.* (2017). <https://doi.org/10.1007/s10973-017-6482-2>
36. I. P. Ejidike and P. A. Ajibade, *Bioinorg. Chem. Appl.* **2015**, 1 (2015). <https://doi.org/10.1155/2015/890734>
37. K. S. Siddiqi, S. A. A. Nami, and Y. Chebude, *J. Braz. Chem. Soc.* **17**, 107 (2006). <https://doi.org/10.1590/S0103-50532006000100016>
38. S. Vellaiswamy G, Ramaswamy, *J. Pharm. Chem. Biol. Sci.* **4**, 153 (2016).
39. S. A. A. Nami, I. Ullah, M. Alam, D. Lee, and N. Sarikavakli, *J. Photochem. Photobiol. B Biol.* **160**, 392 (2016). <https://doi.org/10.1016/j.jphotobiol.2016.05.010>
40. M. S. Iqbal, S. J. Khurshid, and B. Muhammad, *Med. Chem. Res.* **22**, 861 (2013). <https://doi.org/10.1007/s00044-012-0068-0>
41. A. H. Ahmed, A. M. Hassan, H. A. Gumaa, B. H. Mohamed, and A. M. Eraky, *Cogent Chem.* **791**, 1 (2016). <https://doi.org/10.1080/23312009.2016.1142820>
42. M. Ikram, S. Rehman, N. U. Islam, and N. Jan, *J. Mex. Chem. Soc.* **55**, 164 (2011).
43. M. M. E. Shakhofa, M. H. Shtaiwi, N. Morsy, and A. Rasras, *Res. J. Pharm. Biol. Chem. Sci.* **8**, 723 (2017).
44. R. Chandran and S. A. Antony, *Int. J. Pharm. Sci. Res.* **5**, 4339 (2014). [https://doi.org/10.13040/IJPSR.0975-8232.5\(10\).4339-50](https://doi.org/10.13040/IJPSR.0975-8232.5(10).4339-50)
45. J. Akter, A. Hanif, M. S. Islam, M. Haque, S. H. Lee, and L. A. Banu, *Der Chem. Sin.* **8**, 166 (2017).
46. S. A. Elsayed, I. S. Butler, B. J. Claude, and S. I. Mostafa, *Transit. Met. Chem.* **40**, 179 (2015). <https://doi.org/10.1007/s11243-014-9904-z>
47. D. Harikishore, K. Reddy, and S. Lee, *J. Serb. Chem. Soc.* **77**, 229 (2012). <https://doi.org/10.2298/JSC120325099K>
48. F. Asghar, A. Badshah, I. S. Butler, S. Tabassum, B. Lal, and M. N. Tahir, *Inorg. Chim. Acta* **442**, 46 (2016). <https://doi.org/10.1016/j.ica.2015.11.021>
49. P. T. Tuyen, T. D. Xuan, D. T. Khang, A. Ahmad, N. V. Quan, T. T. T. Anh, L. H. Anh, and T. N. Minh, *Antioxidants* **6**, 1 (2017). <https://doi.org/10.3390/antiox6020031>
50. R. J. Wright, K. S. Lee, H. I. Hyacinth, J. M. Hibbert, M. E. Reid, A. O. Wheatley, and H. N. Asemota, *Plants* **6**, 1 (2017). <https://doi.org/10.3390/plants6040048>
51. X. Zhang, Y. Yu, Y. Cen, D. Yang, Z. Qi, Z. Hou, S. Han, Z. Cai, and K. Liu, *Molecules* **23**, 538 (2018). <https://doi.org/10.3390/molecules23030538>